

# Temporal Variation and Reproduction of Microseism H/V Spectral Features in the Osaka Sedimentary Basin with an Irregular-Shaped Interface

H. Uebayashi, H. Kawabe & K. Kamae  
*Research Reactor Institute, Kyoto University, Japan*



## SUMMARY:

Beyond the traditional framework of the one-dimensional velocity structure, the horizontal-to-vertical spectral ratio (HVSr), of microseisms (microtremors with a frequency of about 1 Hz or lower) in areas where the sediment-bedrock interface has irregular topographies, was calculated by finite differential method (FDM)-based simulation. The HVSrs derived from the FDM simulations were both well reproduced in terms of not only the peak frequency (HVfp) but also the spectral curves for complex geological regions. Microseisms originate from the ocean-bottom pressure (the exciting force) characterized by the significant height and period of ocean waves. Therefore, the temporal change of the HVfp and its peak value, of microseism records obtained from spatially different distributions of the amplitude (the power) of the exciting forces scattered in an oceanic region where the investigated area is surrounded, was also reproduced.

*Keywords: Microseisms, H/V spectra, Irregular subsurface structure, Finite different method, Temporal change*

## 1. INTRODUCTION

The studies on reproduction of strong ground motion records based on numerical simulations in sedimentary basin point out that more detailed and precise modelling of three-dimensional (3-D) velocity structures is required to predict strong ground motions with a frequency of about 1Hz or lower, in preparation for the scenario-type earthquakes assumed in earthquake disaster prevention measures. Velocity structure exploration techniques based on the horizontal-to-vertical spectral ratio (HVSr) are extremely useful for acquiring information at a large number of locations to estimate the 3-D velocity structure. Many of the HVSr-based explorations of subsurface structures are performed using a 1-D velocity structural model framework. Even for an irregular subsurface structure, a relatively precise velocity structure model can be constructed in this framework by spatially connecting 1-D velocity structures estimated at different observation sites, provided that the inclination of the sediment-bedrock interface is moderate (e.g. Yamanaka et al. 1994; Delgado et al. 2000; Uebayashi et al. 2008). However, the studies on numerical simulations of microtremors for actual sedimentary basins suggest that the difference between the horizontal-to-vertical spectral peak frequency (HVfp) in a 3-D velocity structure model and the peak frequency of Rayleigh wave ellipticity for the fundamental mode (RHVfp), based on a 1-D velocity structure model below the target area is more than 30–40 per cent in areas where irregular subsurface structures such as ramps and steps exist at the sediment-bedrock interface (Cornou et al. 2004; Guéguen et al. 2007; Uebayashi et al. 2012). In addition, the HVSr peak shape becomes broad or ‘plateau-like’ in the vicinity of an irregular subsurface structure (Uebayashi 2003; Guillier et al. 2006). Thus, it is likely that evaluating the agreement between the HVSr curves and HVfp values derived from observations and those from microseism simulations based on a 3-D velocity structure model would make it possible to identify the velocity structure model for a sediment-bedrock interface with complex topography. In the former of this paper, we attempt to reproduce the observed microseism HVSr curves using the finite difference method (FDM) (Graves 1996) for an Osaka sedimentary basin model, with a focus on areas with irregular subsurface structures and their surrounding areas.

Microtremors are excited by various sources, such as ocean waves and human-related activities. Components with a frequency of 1 Hz or lower, originating from the ocean-bottom pressure (the exciting force) characterized by the oscillation of ocean waves, are specifically called microseisms. Thus, the HVSRs of microseisms in sedimentary basin may be influenced by the distribution profile of the amplitude of ocean waves, since the pressure distribution of atmosphere changes temporally. In the later of this paper, we also attempt to reproduce the temporal change of the HVSRs derived from spatially different distributions of the amplitude (the power) of the exciting forces scattered in an oceanic region where the investigated area is surrounded.

## 2. REPRODUCTION OF HVSR CURVES OF MICROSEISMS IN SEDIMENTARY BASIN

### 2.1. Configuration of the numerical simulation model and the observation sites

In the later chapter, to estimate effect of the distribution spatially biased of the power of the exciting forces scattered in an oceanic region on the HVSRs, the FDM-based microseism simulation was performed for the four (overlapping) regions framed by the grey solid and grey dashed lines in Fig. 2.1. The waveforms in the Osaka sedimentary basin (indicated by bold black box) simulated for each region were superimposed to represent the wavefield of microseisms coming from all directions. Point sources are randomly distributed at a couple of thousands of sites across the ocean area, as indicated by the dots in Fig. 2.1, and correspond to the normal stress on the submarine topography (Marine Information Research Center 2003). The power spectrum of the exciting force is defined as a function of the ocean wave height and the predominant period of ocean waves (Uebayashi 2003). The ocean wave height becomes higher as the distance from the basin increases, as shown by the concentric contour lines in Fig. 2.1. The time history of the exciting force is obtained by inverse Fourier transformation of the above mentioned power spectrum and a phase spectrum based on uniform pseudo-random numbers.

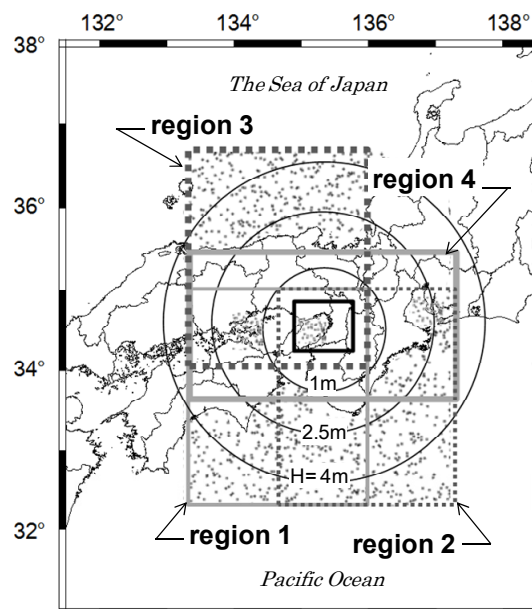


**Figure 2.1.** The position of the Osaka sedimentary basin and the regions for microseism simulation.

The topography of the sediment-bedrock interface in the Osaka sedimentary basin is extremely complicated; the basin structure has been formed through uplift and settling of major several fault zones. The model shown in Fig.2.2 (Yamada & Horike 2007) is unique in that the medium parameters for the sedimentary layer gradually vary as a function of depth, without setting clear geological boundary surfaces. In the microseism numerical simulation, we used an S-wave velocity ( $V_s$ ) of  $0.38 \text{ km s}^{-1}$ , a P-wave velocity ( $V_p$ ) of  $1.60 \text{ km s}^{-1}$  and a density ( $D$ ) of  $1.7 \text{ g cm}^{-3}$  as the lowest stiffness

(uppermost layer) medium parameters and  $V_s$  of  $1.44 \text{ km s}^{-1}$ ,  $V_p$  of  $2.96 \text{ km s}^{-1}$  and  $D$  of  $2.15 \text{ g cm}^{-3}$  as the highest stiffness (lowermost layer) medium parameters in sedimentary layer. The quality factor ( $Q_s$ ) was set to half of  $V_s$  ( $\text{m s}^{-1}$ ). For the medium parameters of the bedrock layer,  $V_s = 2.7 \text{ km s}^{-1}$ ,  $V_p = 5.2 \text{ km s}^{-1}$  and  $D = 2.6 \text{ g cm}^{-3}$  were adopted for the section between depths of 0–3.3 km,  $V_s = 3.2 \text{ km s}^{-1}$ ,  $V_p = 5.8 \text{ km s}^{-1}$  and  $D = 2.7 \text{ g cm}^{-3}$  for the 3.3–12 km section, and  $V_s = 3.4 \text{ km s}^{-1}$ ,  $V_p = 6.0 \text{ km s}^{-1}$  and  $D = 2.8 \text{ g cm}^{-3}$  for the sections below 12 km. In the sedimentary basin region, the grid spacing in the FDM simulation was set to 100 m in the horizontal direction and 50 m in the vertical direction, although it was set to 600 m in both directions in the regions beyond the basin. The theoretical effective frequency range was up to 0.8–1.0 Hz. The calculation was performed for 262 000 steps with a time interval of 0.004 s (corresponding to a total duration of 1048 s). At the same time, the following processes were performed for 840 s, excluding the first 208 s when the response waveforms in the sedimentary basin are transient. The HVSR was evaluated by estimating the power spectra of the three components for 11 sections in total, with each time window being 140 s including a 70-s overlap, and taking an ensemble mean of the HVSR values obtained for the different sections.

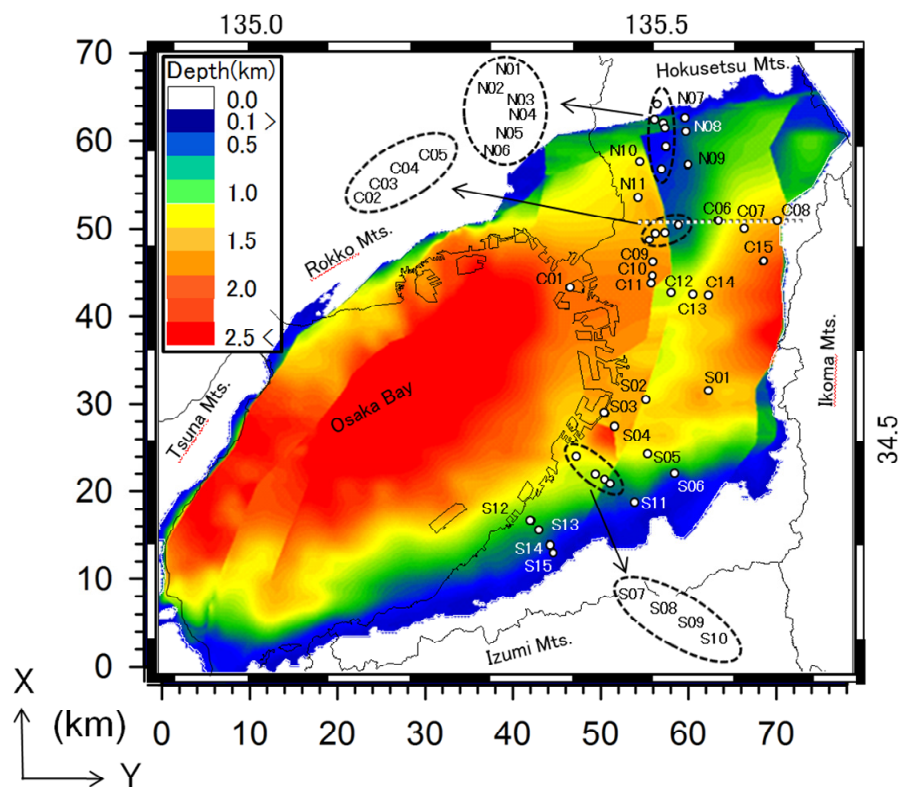


**Figure 2.2.** Distribution of the sediment-bedrock interface depth and microseism observation sites.

Single-station three-component microtremor observations in the Osaka Plain, which occupies the eastern half of the Osaka sedimentary basin, were performed from 2000 to 2010. The observation time for each site ranged from 15 to 30 min. The HVSR was evaluated in a similar way to the microseism simulation process described above. To ascertain the reproduction quality of not only the HVfp but also the HVSR curve that is affected by irregular subsurface structures, we selected the 41 observation sites shown as open circles in Fig. 2.2 with a focus on the areas surrounding the fault zone beneath the Osaka metropolitan area and the edge of the basin.

## 2.2. Reproduction of microseism HVSR features

For the HVSR determined from observations at N03 and N07 in the graben region in the northern region of the Osaka Plain (Fig. 2.3), the FDM simulation successfully reproduced a larger peak value for the east–west component ( $H_{EW}VSR$ ) than for the north–south component ( $H_{NS}VSR$ ), and a lower HVfp for the  $H_{EW}VSR$  than for the  $H_{NS}VSR$ . Moreover, at N03 and N08 in the graben region and at

N10 located immediately west of the Uemachi fault zone, the HVfp derived from the FDM simulation is higher than the RHVfp obtained from Rayleigh wave ellipticity based on a 1-D velocity structure model of the stratigraphic column of the Osaka sedimentary basin model beneath each observation site. In contrast, at N09, away from these areas where the basement depth intricately varies, the HVfp derived from the FDM simulation is fairly consistent with the RHVfp. For the central region of the Osaka Plain, the FDM simulation successfully reproduced a higher peak value in the  $H_{NS}VSR$  than in the  $H_{EW}VSR$  at C03 and C09, located at the top of the footwall side of the Uemachi fault zone. The simulation also reproduced broad peak or no peak shapes of the HVSRs at C04 and C08, situated very close to the Uemachi and Ikoma fault zones. In addition, the HVfp derived from the FDM simulation is higher than the RHVfp at C03 and C04 near the Uemachi fault zone.

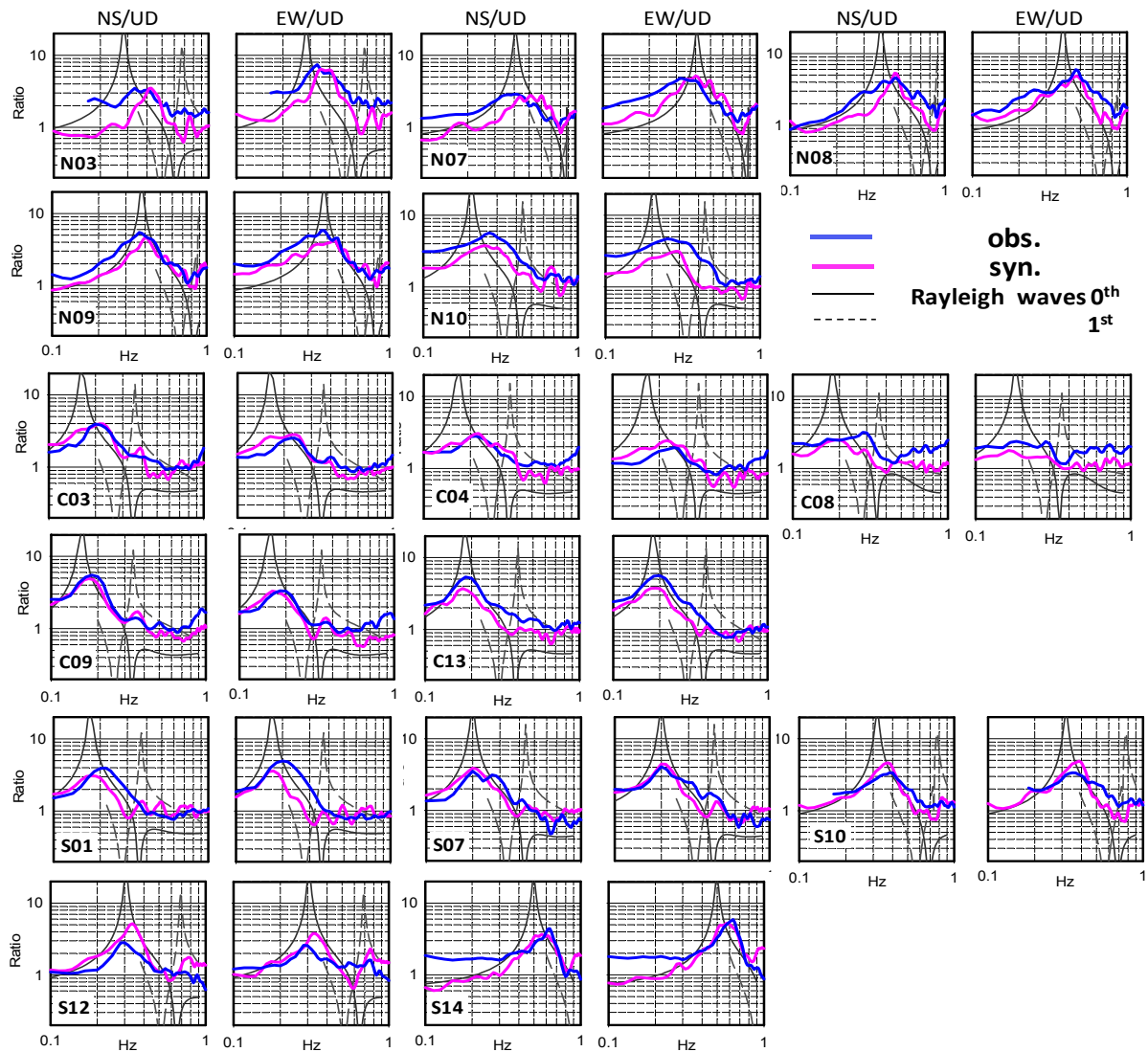


**Figure 2.3.** Comparison of the HVSR curves among the microseism observation, the FDM simulation and Rayleigh wave ellipticity using 1-D velocity structure model, for typical 15 sites.

A general feature of the HVSR in the southern region of the Osaka Plain is that, the HVSR has a sharp peak compared with the northern and the central regions. Also, there was no anisotropy identified in the amplitude of horizontal motions in any azimuth in this region. This is probably because the variation in the basement depth in the region is rather small compared with the other two regions. Incidentally, at S01 and S12, the HVfp differs slightly between the observations and the FDM simulation. This is probably because there is less exploration information on the subsurface structure in this region than for the northern and central regions (Yamada & Horike 2007), and hence the accuracy of the velocity model employed in the FDM simulation was relatively low.

Figure 2.4 shows the correlations for  $H_{NS}$ VSR and  $H_{EW}$ VSR of the HVfps between the observation and the FDM simulation, and between the observation and the Rayleigh wave ellipticity. From the mean values for all sites of the absolute value of the deviation between those peak frequencies described in the figure, it is found that the FDM simulation agrees more than the Rayleigh wave ellipticity in peak frequencies also. From the results shown in this section, for all the regions considered, the FDM simulation reproduced the HVSR extremely well, in terms of not only the fundamental peak frequency but also the spectral curves, which is sensitive to any irregularity in the subsurface structure, and the anisotropy of the amplitude of horizontal motions.

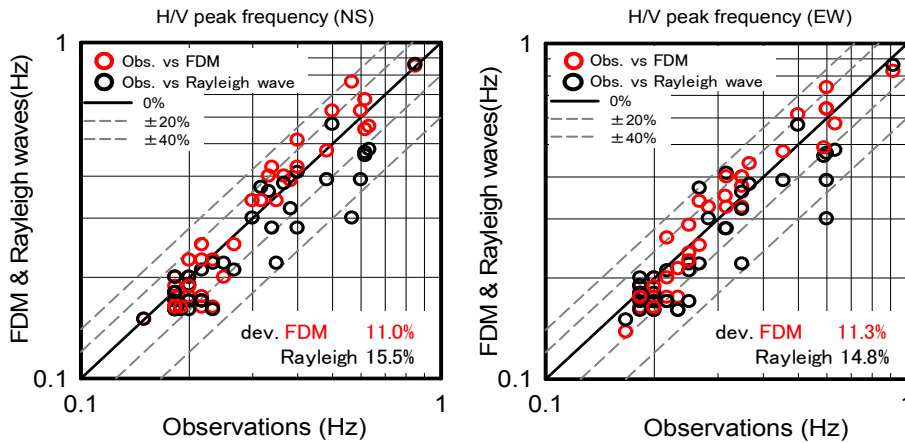


**Figure 2.4.** Correlation of the HVfps for two components between the observation and the FDM simulation, and between the observation and the Rayleigh wave ellipticity.

### 2.3. Relation between the HVSR features (peak frequency and its value) and the topographies

The fundamental peak value and its peak frequency of the HVSR in the Osaka sedimentary basin model were overviewed in this section. The fundamental peak of the HVSR obtained by composing the two horizontal components ( $H_{rms}$ VSR) was evaluated for peak values of 2.0 and higher. As shown in Fig. 2.5, the peak value of the  $H_{rms}$ VSR exceeds 5 in the Senri hills located in the northern region of the Osaka Plain, and the southern region where the sediment-bedrock interface is slightly inclined, whereas it is below 4 in the oceanfront area of Osaka Bay in the central region. The S-wave velocity ratio of the sedimentary layer obtained by averaging the medium parameters to the bedrock becomes 0.2–0.35. In the ranges, the peak value increases in a place (a region where the sedimentary layer is thin, such as Senri hills and the southern region of the Osaka Plain described above) where the velocity ratio is low (in other words, the velocity contrast is high), and the peak value decreases in a place (a region where the sedimentary layer is thick in the Osaka Bay) where the velocity ratio is high (the contrast is low) (Tuan et al. 2011). However, in the vicinity of the steps on the sediment-bedrock interface along the Uemachi fault zone and the edge of the basin, the peak value is notably low (3 or lower) compared with the surrounding areas, over an extensive range. This implies that a step structure of an unknown sediment-bedrock interface (or a dip-slip fault) may be estimated based on microtremors, by finding an area where the peak value sharply drops within a narrow range in the sedimentary layer.

In the correlation between the spatial variation of the peak frequencies obtained by the two approaches shown in Fig. 2.6 and the basement depth (Fig. 2.2), the HVfp (obtained by composing the two horizontal components) derived from the FDM simulation is lower than the RHVfp obtained from Rayleigh wave ellipticity. Figure 2.7 presents the residuals between the peak periods (reciprocal of the peak frequencies shown in Fig. 2.6) obtained by the two approaches, with respect to the value for Rayleigh wave ellipticity. Regions where the absolute value of the residual is large correspond to areas where the basement depth sharply changes. This means that it is difficult to estimate complex geological conditions such as step structures with high resolution for a sediment-bedrock interface, based solely on the HVfp derived from observations. Therefore, it is necessary to evaluate not only the peak frequency but also how well the HVSR peak values fit.

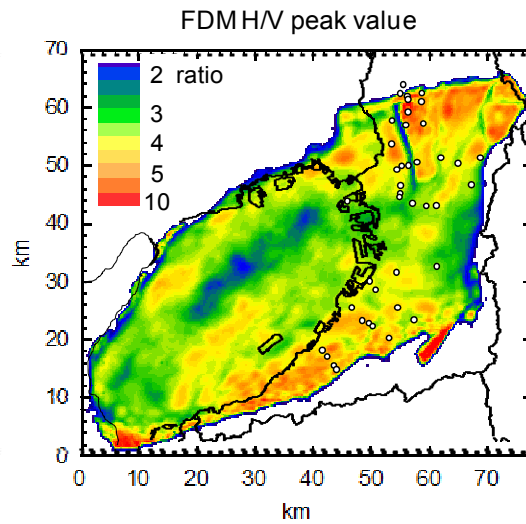


Figure 2.5. Distribution of the HVSR peak values obtained from the FDM simulation.

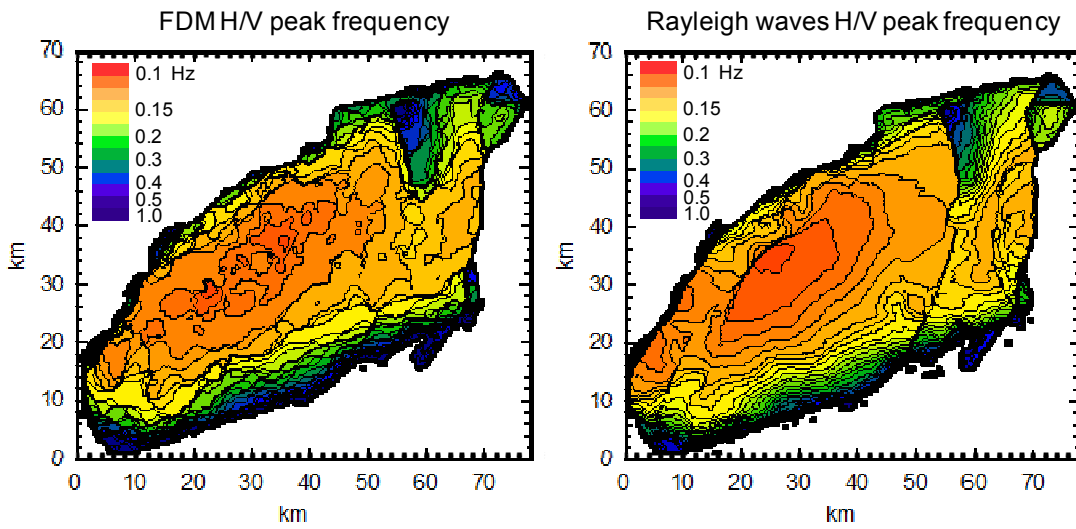


Figure 2.6. Comparison of the distribution of the HVSR peak frequencies between the FDM simulation and the Rayleigh wave ellipticity.

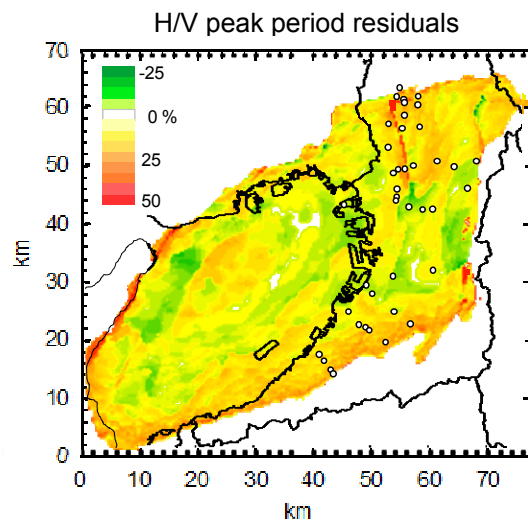


Figure 2.7. Residual distribution of the peak periods between the FDM simulation and Rayleigh wave ellipticity.

### 3. THE EFFECT OF THE DISTRIBUTION SPATIALLY BIASED OF THE POWER OF EXCITING FORCE ON HVSR

#### 3.1. Temporal change of the HVfp and its peak value at site S01

Single-station continuous microtremor observation was performed from 6th to 8th of Sept., 2005 at site S01 located in the south-eastern region of Osaka plains. The ocean-wave height distribution around Japan Island has been changing dramatically during the observation period, because the typhoon passed over the Japan Island. This means that the spatially distribution of the power of the exciting forces as the origin of microseisms changes temporally. Figure 3.1 shows a temporal change of the HVfps and its peak values at S01 for the three days. The HVfps and its peak values have a negative correlation as shown in the figure. The range of those variations for the transitional period of the ocean-wave amplitude distribution is approximately 15% for the HVfp and approximately 70% for the peak value. On the other hand, those ranges for the periods when the change of the ocean-wave amplitude distribution is gradual are approximately 10% and 20%, respectively. This phenomenon suggests that in modeling of velocity structures using the HVSR, the use of the microseism records measured for the transitional period of the ocean-wave amplitude distribution is undesirable.

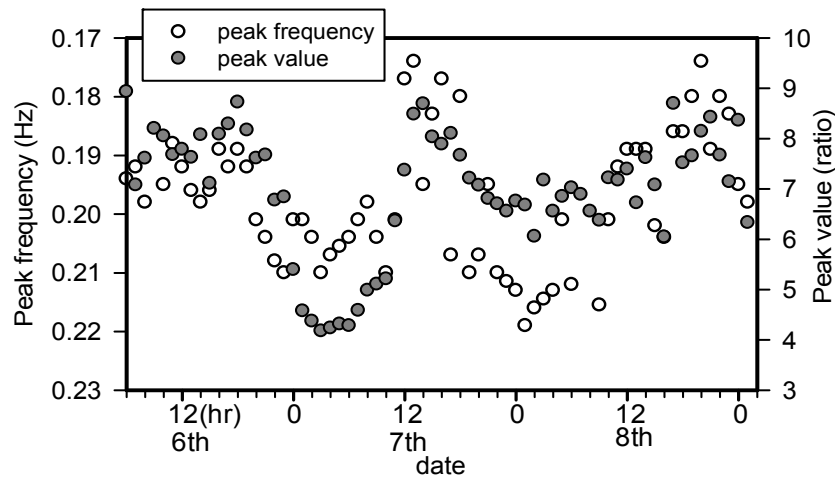


Figure 3.1. Temporal change of the HVfps and its peak values at S01 for the three days.

#### 3.2. Simulation of the temporal change of the HVSR

To reproduce the temporal change of the HVfp and its peak value at S01, the HVSR derived from synthetic microseisms simulated using four different distributions of the power of the exciting forces scattered in the oceanic region around the Osaka sedimentary basin is calculated. The coefficients shown in Table 3.1 mean the weight multiplied to the power spectrum of exciting forces described above. The case A represents the distributions with the even power of the exciting forces for all azimuths, whereas in other cases, the distributions of the power are deflected. With respect to the degree of the change of the HVfp and its peak value, the observation is consistent with the results of the FDM simulation as shown in Fig. 3.2. Spatial distributions of the difference of the HVfp and its peak value between the case A and the other are shown in Figs. 3.3 and 3.4, respectively. Those differences are determined by subtracting the result of the other from the case A and dividing the result of the case A. Considering the relationships between those distributions and the arrival directions of predominant microseism amplitude (resulting from the distributions of the power of the exciting forces) corresponding to each of the cases B-D, it is suggested that the HVfp and its peak value are influenced by the velocity structure in the propagation path of predominant microseism components.

To examine the variation ranges of the HVfp at various sites, a difference of the HVfp between the case A and the other is shown in Fig. 3.5. The coefficient of variation in each case is 11 to 25%. As a common feature of the three figures, biases in the low frequency are larger than that in high frequency.

**Table 3.1.** Contribution (weight coefficient) of the sources in the four regions (see Fig.1) to synthetic microseisms using the HVSr processing.

	region 1	region 2	region 3	region 4
case A	1.0	1.0	1.0	0.5
case B	1.0	1.0	0.5	0.3
case C	0.5	0.5	1.0	0.5
case D	1.0	0.5	0.5	1.0

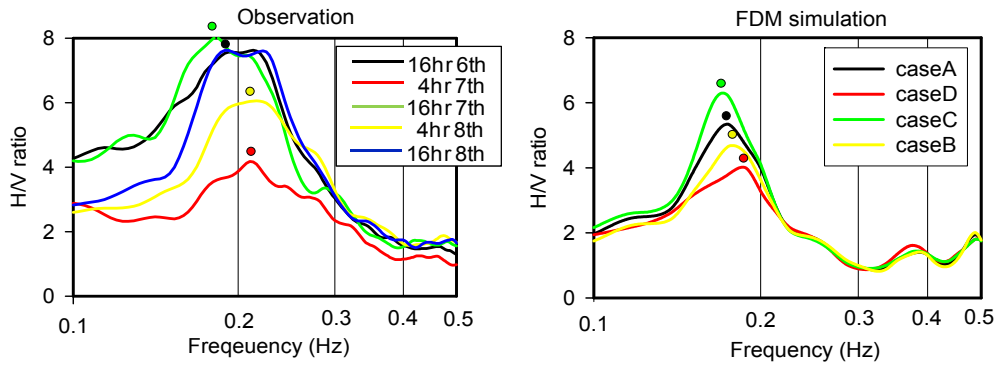


**Figure 3.2.** Comparison of the degree of the change of the HVfps and its peak values at site C01 between the observation and the FDM simulation.

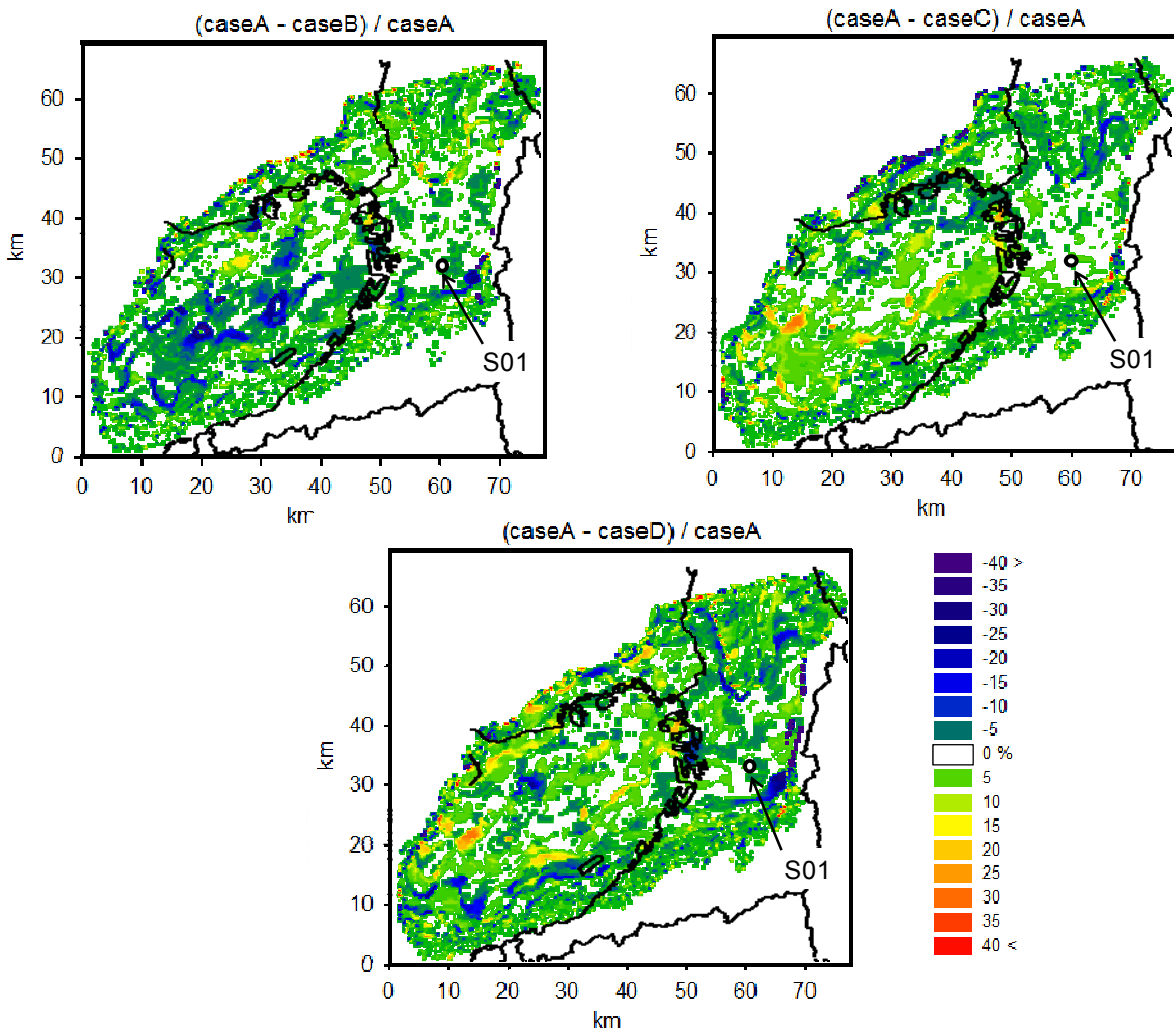


**Figure 3.3.** Residual distribution of the HVfp between the case A and the other (cases B, C and D).



## 4. CONCLUSIONS

For the Osaka sedimentary basin, which has a sediment-bedrock interface with complex 3-D topographies, the reproduction of the HVSR curve of microseisms with a period of 1 s or more obtained from observations was performed by using 3-D FDM simulations. Moreover, the effect of the distribution spatially biased of the power of the exciting forces scattered in an oceanic region on the HVSRs was estimated. The following results were obtained. With respect to the HVSR curves, the results of the FDM simulation and the observation agreed well even in areas with strong irregularities in the geological structures of the sediment-bedrock interface. With respect to the HVSR peak frequencies, the mean values for all observation sites of the deviation between the observation and the FDM simulation, and between the observation and the Rayleigh wave ellipticity are about 11 per cent and 15 per cent, respectively. The temporal change of the HVfp and its peak value of microseisms at a period into which the ocean-wave height distribution around Japan Island dramatically changed was also reproduced by the FDM simulations using spatially biased distributions of the power of the exciting forces scattered in an oceanic region. In addition, those HVfp and its peak value are influenced by the velocity structure in the propagation path of predominant microseism components.

## ACKNOWLEDGEMENT

This study was supported in part by Grants-in-Aid for Scientific Research (C) (Numbers 20560540 and 23560670) from Japan Society of the Promotion Science.

## REFERENCES

- Cornou, C., Kristek J., Ohrnberger, M., Giulio D. G., Schissele E., Guillier, B., Bonnefoy-Claudet, S., Wathelet, M., Fäh, D., Bard, P.-Y., & Moczo, P. (2004). *Simulation of seismic ambient vibrations-II H/V and Array techniques for real sites*, in **Proc. 13th World Conf. Earth. Engng., Vancouver, BC, Canada**, paper 1130.
- Graves, R.W., (1996). *Simulating seismic wave propagation in 3D elastic media using staggered-grid finite differences*, **Bull. Seism. Soc. Am.** **86**, 1091-1106.
- Delgado, J., Casado, C.L., Giner, J., Estévez, A., Cuenca, A. & Molina, S. (2000). *Microtremors as a geophysical exploration tool: applications and limitations*, **Pure appl. Geophys.**, **157**, 1445–1462.
- Guéguen, P., Cornou, C., Garambois, S. & Banton, J. (2007). *On the limitation of the H/V spectral ratio using seismic noise as an exploration tool: application to the Grenoble Valley (France), a small apex ratio basin*, **Pure Appl. Geophys.** **164**, 115-134.
- Guillier, B, Cornou, C., Kristek, J., Moczo, P., Bonnefoy-Claudet, S., Bard, P.-Y. & Fäh, D. (2006). *Simulation of seismic ambient vibrations: does the H/V provide quantitative information in 2D-3D structures?*, in **Proc. 3rd. Int. Symp. on the Effects of Surface Geology on Seismic Motion**, Grenoble, France, Paper 185.
- Marine Information Research center, (2003). *Japan Hydrographic Association, JTOPO30, M1406 & M1407*.
- Tuan, T. T., Scherbaum F. & Malischewsky P. G., (2011). *On the relationship of peaks and troughs of the ellipticity (H/V) of Rayleigh waves and the transmission response of single layer over half-space models*, **Geophys. J. Int.**, **184**, 793-800.
- Uebayashi, H., (2003). *Extrapolation of irregular subsurface structures using the horizontal to vertical spectral ratio of long period microtremors*, **Bull. Seism. Soc. Am.**, **93**, 570-582.
- Uebayashi, H., Kawabe, H., Kamae, K. & Miyakoshi, K., & Horike, M., (2008). *Robustness of microtremor H/V spectra in the estimation of an inclined basin-bedrock interface and improvement of the basin model in Southern part in Osaka plains.*, **J. Struct. Constr. Eng., AIJ**, **74**, 1453-1460. (in Japanese with English abstract).
- Uebayashi, H., Kawabe & H., Kamae, (2012). *Reproduction of microseism H/V spectral features using a three-dimensional complex topographical model of the sediment-bedrock interface in the Osaka sedimentary basin*, **Geophys. J. Int.**, **189**, 1060-1074.
- Yamada, K. & Horike, M., (2007). *Inference of Q-Values below 1 Hz from borehole and surface data in the Osaka basin by three-component waveform fitting*, **Bull. seism. Soc. Am.**, **97**, 1267–1278.
- Yamanaka, H., Takemura, M., Ishida, H. & Niwa, M., (1994). *Characteristics of long-period microtremors and their applicability in exploration of deep sedimentary layers*, **Bull. seism. Soc. Am.**, **84**, 1831–1841.